MOLECULAR GAS IN ULTRALUMINOUS INFRARED GALAXIES

P. M. SOLOMON
Astronomy Program, SUNY, Stony Brook
Stony Brook, N.Y. 11794-2100

1. Introduction

The discovery of CO emission (Wilson, Jefferts & Penzias 1970) 25 years ago opened a major new astronomical window which has led to important advances in many areas of Galactic and extragalactic astronomy. The strength and ubiquity of the CO lines, CO isotopic lines, and other millimeter transitions have provided extraordinary diagnostics for studying molecular interstellar matter in the Milky Way and in external galaxies. All dense interstellar gas is molecular hydrogen, H_2 (Solomon & Wickramasinghe 1969), due to the sharp transition from H I to H_2 caused by the self-shielding of H_2 from photodissociation by absorption in the Lyman bands followed by emission downward into the continuum. The balance between formation on grains and photodissociation yields an optically thick self-shielding layer in all clouds where the total neutral hydrogen density $n(\mathrm{H} + 2\mathrm{H}_2) > 100$ cm^{-3}. Since H_2 itself has no radio or millimeter transitions and H I is absent, abundant minor constituents like CO become the main tracer of H_2. All current star formation takes place in molecular clouds since the first stage of star formation is the formation of high-density interstellar clouds. Molecular clouds and particularly giant molecular clouds (GMC), with masses $> 1 \times 10^5$ $M_\odot$, the most massive objects in the Galaxy are a major component of the interstellar medium.

My assignment from the organizers is to discuss molecular clouds in the context of extragalactic observations. Presumably, this involves an analysis of the differences and similarities between Milky Way GMCs and the sources of millimeter lines from CO and other molecules in galaxies near and far. Within the confines of a 15 minute talk this is a difficult task but the real problem is more fundamental. There are only a few extragalactic molecular clouds observed with sufficient angular resolution to determine their morphology or dynamical mass and these are in a few of the nearest galaxies where the resolution is very marginal compared with the size of individual clouds. Therefore, many important physical properties of molecular clouds, including their mass, size distribution, and average densities cannot be directly determined for extragalactic GMCs. Since most extragalactic clouds cannot be imaged, observations pertain to the ensemble of clouds in a galaxy and indirect measurements including line ratios, use of high-density tracers, and large scale morphology must be used to deduce the physical properties of the molecular ISM. Section 2 discusses the evidence for gravitationally bound molecular clouds in the Milky Way. Milky Way observations are a reasonable foundation for studying clouds in the disks of spiral galaxies. Section 3 presents observations and interpretation of molecular emission from ultraluminous IR galaxies with extremely different physical conditions from clouds in the disk of the Milky Way.

2. Gravitationally Bound Giant Molecular Clouds

The physical basis for the use of CO as a quantitative tracer of H_2 rests on the origin of the emission from gravitationally bound molecular clouds (Dickman et al. 1986; Solomon et al. 1987). For a single cloud or an ensemble of non-overlapping, virialized gas clouds, the gas mass $M_{\rm gas}$, and CO line luminosity $L_{\rm CO}$, are linearly related by the quantity α given by

$$M_{\rm gas} /\ L_{\rm CO} = \alpha = \left(\frac{4\,\mu 1.36}{3\,\pi\, G}\right)^{1/2} \frac{n^{1/2}}{T_{\rm b}} \ = \ 2.6\ \frac{n^{1/2}}{T_{\rm b}}, \qquad (1)$$

where μ is the mass of an H_2 molecule (helium adds 36% by mass), $n[{\rm cm}^{-3}]$ is the volume averaged H_2 number density in the clouds, and $T_{\rm b}$[K] is the intrinsic (rest frame) brightness temperature of the CO(1–0) line. $M_{\rm gas}$ is given in units of $M_\odot$ and $L_{\rm CO}$ in units of in ${\rm K\,km\,s^{-1}\,pc^2}$.

For gravitationally bound clouds the mean density n is determined by the size and velocity linewidth. Maloney (1990) has claimed that the correlation between CO luminosity and virial theorem mass determined directly form size and linewidth measurements is an artifact of the size-linewidth relation and does not prove that molecular clouds are virialized. Maloney repeated the derivation of the observed virial mass from the size-linewidth relation given by Solomon et al. (1987) and turned the argument upside down by suggesting that any size-linewidth relation would produce a virial mass-CO luminosity relation, even if the clouds were not virialized. This argument misses the point and ignores the physics involved in the various methods of mass determination. The strong evidence for gravitationally bound clouds is not the simple correlation between virial mass and CO luminosity; it is (Solomon et al. 1987) the agreement between the absolute value of the virial mass and the mass determined by completely different and totally independent techniques. The dynamical (virial) mass determined for Galactic molecular clouds agrees well with the "luminosity mass" determined from CO line luminosities and integrated intensities calibrated by γ ray measurements and also by comparison of ^{13}CO intensities with extinction in nearby dark clouds. Indeed, for massive molecular clouds the dynamical mass and the luminosity mass agree in general to within a factor of 2. One of these methods involves the use of Newton's gravitational constant G, the other two involve star counting techniques combined with optically thin column densities and the comparison of γ rays from molecular and atomic regions. It is not an accident that these 3 techniques basically agree. If molecular clouds were not gravitationally bound the virial mass would turn out wildly different from the CO luminosity mass, as is the case for unbound sources such as outflows from young stars. There is no "dark matter" in molecular clouds. Most of the mass in the molecular ISM is at the high end of the mass spectrum. While there are obviously many small clouds, including "high latitude clouds," and some of them are not gravitationally bound, they do not contribute significantly to the total molecular mass (Heithausen et al. 1993).

3. CO Emission from Ultraluminous Infrared Galaxies

We have carried out a systematic CO(1–0) survey (Solomon et al. 1996) with the IRAM 30 m telescope of a large sample of ultraluminous galaxies out to $z = 0.27$. This is part of a multi-line study with a goal of understanding the difference between the star-forming environment in ultraluminous galaxies and spiral galaxies like the Milky Way. A second stage of this investigation involves imaging about 10 galaxies with the IRAM Interferometer (Downes & Solomon 1996). Ultraluminous galaxies, with IR luminosities $> 10^{12}\,L_\odot$ (cf. Sanders et al. 1988), are the most luminous objects in the local universe. The brightest (nearest) ten ultraluminous galaxies (Sanders et al. 1988) are all either merging systems or have tails indicating a recent merger. Besides the very large IR luminosity, the molecular interstellar medium in such galaxies differs from that in normal spiral galaxies in several fundamental respects. First, although these galaxies have high CO luminosities and molecular masses, the ratio of far-infrared to CO luminosity is about an order of magnitude greater than for normal spiral galaxies (e.g., Sanders et al. 1986; Solomon & Sage 1988). In star formation models, this implies a much higher star formation rate per solar mass of molecular gas than in normal galaxies, even gas rich spirals. Second, a large fraction of their molecular mass is at densities much higher than in ordinary giant molecular clouds, as shown by HCN observations which trace gas at densities $> 10^5\,\mathrm{cm}^{-3}$ (Solomon, Downes & Radford 1992). In nearby ultraluminous galaxies, direct interferometric measurements (e.g., Scoville et al. 1991; Radford et al. 1991) show most of the CO, HCN, and molecular mass is concentrated in a small central region (less than 1 kpc). Indeed, estimates of the molecular mass in the central condensation often equal the dynamical mass (e.g., Scoville et al. 1991). This conflict between dynamical mass and H_2 mass derived from CO luminosity leads to a new interpretation of the CO luminosity (Downes, Solomon & Radford 1993; hereafter DSR) for a medium which may fill a disk or sphere in the central few hundred parsecs of a galaxy.

3.1. CO SURVEY OBSERVATIONS

The sample of 37 sources includes a large fraction of the most luminous IRAS galaxies in the northern sky. Of the ten most luminous galaxies in the optical redshift survey (Strauss et al. 1992) above $\delta > -10°$, our sample includes eight. Twenty galaxies in our sample are more luminous than the prototype IR galaxy Arp 220. The most luminous object in the sample, 14070+0525 with $4\times10^{12}\,\mathrm{L}_\odot$ in the far IR, is also the most distant. Figure 1 shows some sample CO spectra and R band images (full data are presented in Solomon et al. 1996).

All of the candidate galaxies, without exception, have high CO luminosities and a high infrared to CO luminosity ratio. Figure 2 is a diagram of FIR luminosity vs. CO luminosity for the galaxies in our sample. For comparison, a well-known galaxy and the trend for normal and weakly interacting spirals (Solomon & Sage 1988) are also shown. For ultraluminous galaxies (but not in general for other or normal galaxies) the CO integrated line intensity, I_{CO}, is tightly correlated with $100\,\mu$m flux density (Fig. 3). In order to explain the high IR to CO luminosity ratio and the tight CO – $100\,\mu$m correlation we (DSR; Solomon et al. 1996) have developed a "black body" model which predicts a high ratio and shows there is a clear upper limit to $L_{\mathrm{FIR}}/L_{\mathrm{CO}}$. The most luminous galaxies are very near this limit. This implies the dust is optically thick even in the far IR (see also Condon et al. 1991), and that the ratio is not a simple indicator of luminosity to molecular mass. The model also leads to a re-interpretation of the molecular mass determination for ultraluminous galaxies.

3.2. THE BLACK–BODY MODEL

We assume the CO traces a huge cloud of area filling factor unity and the dust is opaque for $\lambda \leq 100\,\mu$m. The source may be a disk, a torus, a bar, or have an irregular shape. For illustration, we derive the luminosity ratio for

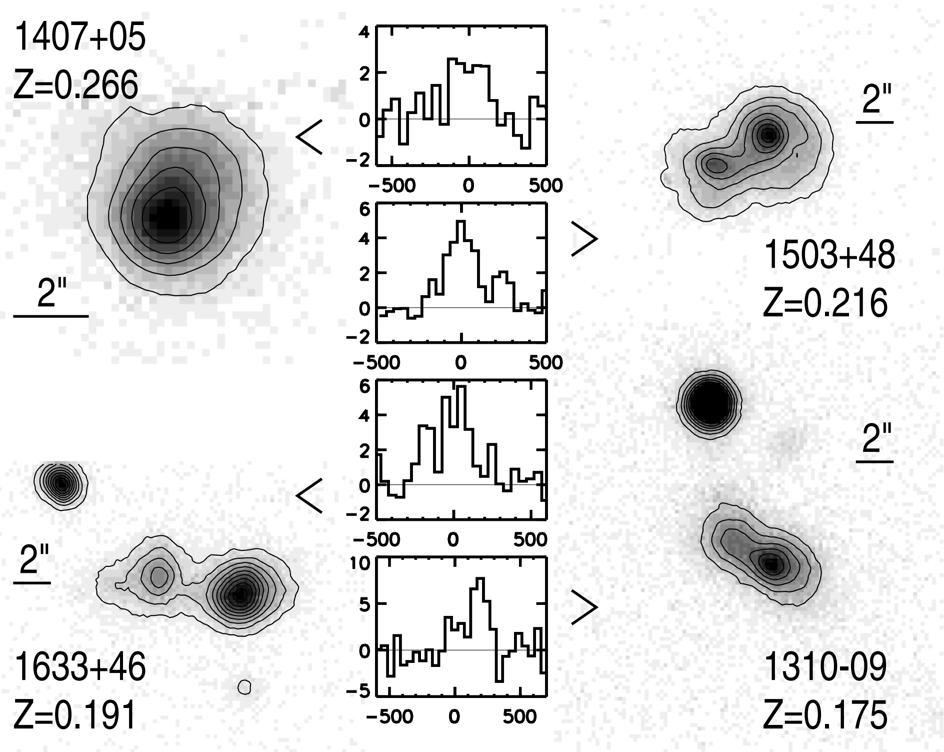

Figure 1. Sample IRAM 30 Meter CO Spectra and R band CCD images of ultraluminous galaxies. North is at the top, East is to the left. Next to each image is source name, redshift and CO(1–0) spectrum, with intensity in milliKelvin (from Solomon et al. 1996). The images were taken at the Univ. of Hawaii 3.5 m telescope by Sanders & Kim (1993, priv. communication).

a sphere, but as long as the CO and far IR sources cover the same area, the FIR/CO luminosity ratio is independent of source shape. For an optically thick sphere of temperature T_d at its outer radius R,

$$L_{\rm FIR} = 4\,\pi\,R^2\,\sigma\,T_d^4 \quad , \tag{1}$$

where σ is the Stephan-Boltzmann constant. Similarly, the CO(1–0) luminosity

$$L_{\rm CO} = 4\,\pi^2\,R^2\,\frac{2\,k}{\lambda^2}\int T_b\,d\nu \quad , \tag{2}$$

where T_b is the intrinsic brightness temperature, ν is frequency, and $L_{\rm CO}$ is in the same units as $L_{\rm FIR}$ (e.g., Watts or $L_\odot$). We assume that regardless of how the gas is clumped in volume, the region has an area filling factor of unity. The temperatures are determined from the far IR colors. If $T_b = T_d$,

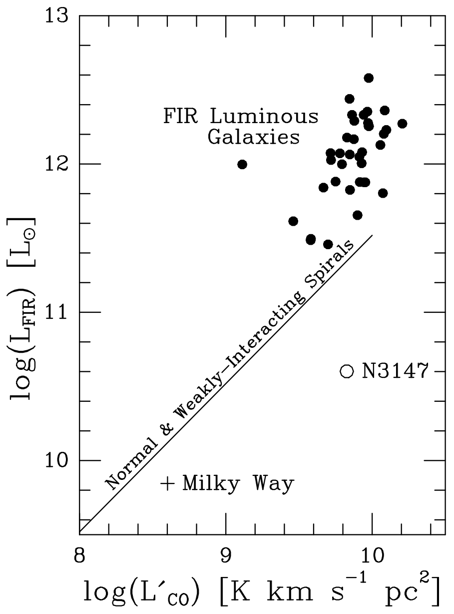

Figure 2. FIR luminosity vs. CO(1–0) luminosity (lower scale) and molecular gas mass (top scale). Solid circles indicate galaxies in our sample. Normal and weakly interacting spirals are scattered about the solid line. Open circles show locations in this diagram for one well-known galaxy (from Solomon et al. 1996).

$$\frac{L_{\rm FIR}}{L_{\rm CO}} \;=\; \frac{\sigma\, T_d^3\, c^3}{2\,\pi\, k\, \nu_{\rm CO}^3\, f_V\, \Delta V} \quad , \tag{3}$$

where $\nu_{\rm CO}$ is the CO(1–0) rest frequency, f_V the velocity filling factor, and ΔV the linewidth. For typical values,

$$\frac{L_{\rm FIR}}{L_{\rm CO}} \;=\; 4.8\times 10^6 \left(\frac{T_d}{50K}\right)^3 \left(\frac{300}{f_V\, \Delta V}\right) \quad . \tag{4}$$

$$\frac{L_{\rm FIR}}{L_{\rm CO}} \;=\; 4.8\times 10^6 \left(\frac{L_{\rm FIR}}{10^{12}\, L_\odot}\right)^{3/4} \left(\frac{300\ {\rm pc}}{R}\right)^{3/2} \left(\frac{300}{f_V\, \Delta V}\right) \quad . \tag{5}$$

With the CO luminosity in $\rm K\,km\,s^{-1}\,pc^2$,

$$L'_{\rm CO} \equiv \pi\, R^2\, T_b\, f_V\, \Delta V \quad , \tag{6}$$

the ratio becomes

$$\frac{L_{\rm FIR}}{L'_{\rm CO}} \;=\; 224 \left(\frac{T_d}{50K}\right)^3 \left(\frac{300}{f_V\ \Delta V}\right) \quad , \tag{7}$$

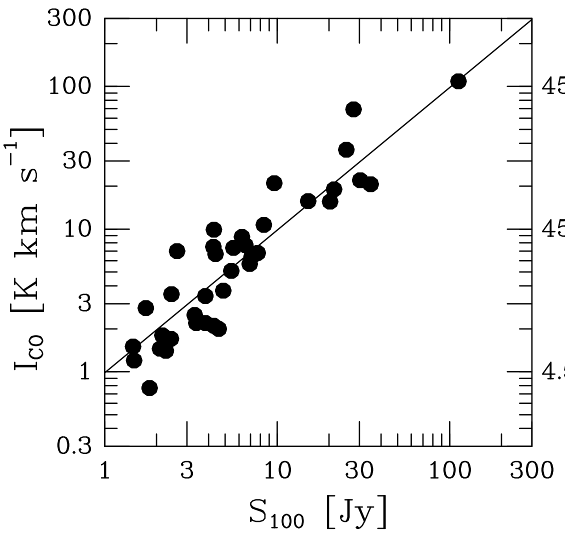

Figure 3. Integrated CO(1–0) line intensity vs. IRAS 100 μm flux density for the ultraluminous galaxies in our sample. The solid line corresponds to the relation $I_{\rm CO} = 1.0 \times S_{100}$ (from Solomon et al. 1996).

where the $L_{\rm FIR}/L'_{\rm CO}$ ratio now has units of $\rm L_{\odot}$ $(\rm K\,km\,s^{-1}\,pc^2)^{-1}$.

Figure 4 shows that the most luminous galaxies are within a factor of 2 of the black body limit. We can use this model to derive sizes of the FIR and CO emitting regions and the enclosed dynamical masses. Much of the IR and CO emission originates in regions several hundred parsecs in radius. The entire ISM is a scaled up version of a normal galactic disk with the ambient densities a factor of 100 higher, making even the intercloud medium a molecular region. Normal GMCs are not the source of CO emission in this environment.

The dynamical masses are typically a factor of 3 below the H_2 mass obtained from the use of a Milky Way conversion factor. Under conditions where the CO emission is from a filled medium in the center of a galaxy and not from an ensemble of individual bound clouds, the CO luminosity measures the geometric mean of the dynamical and H_2 (gas) mass

$$M_{\rm dyn} M({\rm H_2}) = (\alpha\, L'_{\rm CO})^2 \quad . \tag{8}$$

H_2 masses determined from the assumption of optically thin CO emission yield lower limits about a factor of 3 below the dynamical mass.

Figure 4. The distant-independent quantity $L_{\mathrm{FIR}}/L_{\mathrm{CO}}$ vs. the far IR black body dust temperature derived from the IRAS flux ratio S_{60}/S_{100}. The line indicates the upper limit for the luminosity ratio for the black body model in eq.(7), with $f_V\,\Delta V = 300\,\mathrm{km\,s^{-1}}$. Solid circles: galaxies in our sample with $L_{\mathrm{FIR}} > 10^{12}\,\mathrm{L}_\odot$. Open circles: galaxies with $L_{\mathrm{FIR}} < 10^{12}\,\mathrm{L}_\odot$ (from Solomon et al. 1996).

4. HCN and CS: Dense Gas in Ultraluminous Galaxies

The centers of ultraluminous galaxies exhibit several other important differences from normal spiral galaxies. Most important is the extremely high HCN luminosity. HCN traces H_2 at a much higher density ($\sim 10^5$ cm^{-3}) than CO (~ 500 cm^{-3}). The HCN luminosities of the ultraluminous galaxies Mrk 231, Arp 193, Arp 220, and NGC 6240 are greater than the CO luminosity of the Milky Way (Solomon, Downes & Radford 1992). They have $\sim 10^{10}$ $\mathrm{M}_\odot$ of H_2 at a density $> 10^4$ cm^{-3}, about 300 times the mass of dense H_2 in the Milky Way. The ratio of HCN to CO luminosity is 1/7 to 1/4 for ultraluminous galaxies, but only 1/30 or less in the disks of normal spiral galaxies. CS emission is also present but at an intensity about a factor of 3 less than HCN. A large fraction of the molecular gas in ultraluminous galaxies, perhaps 50%, is in very dense regions similar to star forming cloud cores, rather than in the envelopes of giant molecular clouds. Thus, the density of molecular clouds in ultralumious galaxies is much higher than Milky Way GMCs. The ratio of far-infrared to HCN luminosity is similar for ultraluminous galaxies and for normal spirals, including the Milky Way, which suggests that the star formation rate per mass of *dense* gas is independent of the infrared luminosity or the state of interaction. The molecular gas density in the central regions of the ultraluminous galaxies ($\sim$500 $M_\odot$ pc^{-3}) is similar to the stellar density in the centers of elliptical galaxies, consistent with the idea that some mergers may eventually become ellipticals.

5. ^{13}CO Observations of Ultraluminous galaxies

The brightness temperature ratio of ^{13}CO to ^{12}CO in ultraluminous galaxies is extremely low (Solomon, Downes & Radford 1996). Our observations show that for Arp220, NGC 6240 and Mrk231 this ratio is in the range of 1/50 to 1/30, instead of the typical 1/10 in spiral galaxy disks. This indicates that CO emission has lower optical depth than in galactic disks, or ^{13}CO is less abundant relative to ^{12}CO, or both. Again, the physical conditions are very different for Milky way GMCs and a full interpretation requires a broad based multi-line study. The cores of ultraluminous galaxies are the sites of the most extreme molecular environments with very dense clouds, and an intercloud medium emitting much of the CO and ^{13}CO emission.

6. IRAS F10214+4724: A Lensed Ultraluminous Galaxy at z=2.3

In the past few years, through the combination of improved technology and a boost from gravitational lensing, it has become possible to observe CO emission from ultraluminous galaxies at high redshift. An example is F10214+4724 shown in Figure 5 (Downes, Solomon & Radford 1995). By combining information from Keck telescope K band images and IRAM interferometer CO images, it is possible to deduce the magnification factor for the CO emission. The resulting intrinsic CO luminosity, IR luminosity and size are very similar to that of local ultraluminous IR galaxies.

References

Condon, J.J., Huang, Z.P., Yin, Q.F., & Thuan, T.X. 1991, *ApJ*, **378**, 65.
Dickman R.L., Snell, R.L., & Schloeb, F.P. 1986, *ApJ*, **309**, 326.
Downes, D. & Solomon, P.M. 1996 (to be published).
Downes, D., Solomon, P.M., & Radford, S.J.E. 1995, *ApJ*, **453**, L65.
Downes, D., Solomon, P.M., & Radford, S.J.E. 1993, *ApJ*, **414**, L13 (DSR).

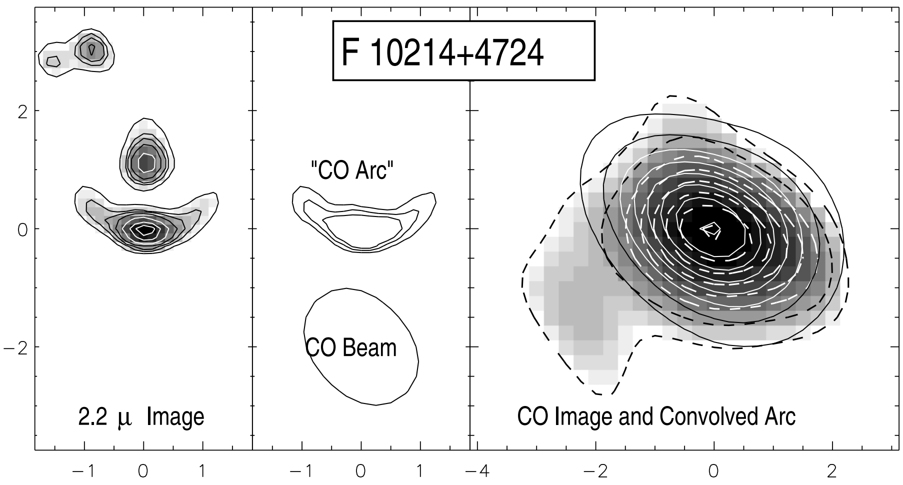

Figure 5. CO arc and image from 10214+4724 at z = 2.3. Offsets are in arcseconds. Left: Keck telescope 2.2 μm image. The feature north of the arc is the lensing galaxy and the other features are unrelated (Matthews et al. 1994). Middle: Truncated 2.2 μm image used to model the CO arc and the half power shape of the IRAM interferometer beam. Right: IRAM interferometer CO map in gray scale and dashed contours. Solid contours are the model image obtained by convolving the beam with the arc. The fit is very good, and the difference between the observed image and the model has the same rms noise as the original map. The CO magnification is a factor of 5 to 10 (Downes, Solomon & Radford 1995).

Heithausen, A., Stacy, J.G., deVries, H.W., Mebold, U., & Thaddeus, P. 1993, *A&A*, **268**, 265.
Maloney, P. 1990, *ApJ*, **348**, L9.
Matthews, K., et al. 1994, *ApJ*, **420**, L13.
Radford, S.J.E., et al. 1991, in Dynamics of Galaxies and Their Molecular Cloud Distributions, ed. F. Combes & F. Casoli (Dordrecht: Kluwer), 303.
Sanders & Kim 1993 (priv. comm.)
Sanders, D.B., Soifer, B.T., Elias, J.H., Madore, B.F., Matthews, K., Neugebauer, G., & Scoville, N.Z. 1988, *ApJ*, **325**, 74.
Sanders, D.B., et al., 1986, *ApJ*, **305**, L45.
Scoville, N.Z., Sargent, A.I., Sanders, D.B., & Soifer, B.T. 1991, *ApJ*, **366**, L5.
Solomon, P.M., Downes, D., Radford, S.J.E., & Barrett, J.W. 1996 (to be published in ApJ).
Solomon, P.M., Downes, D., & Radford, S.J.E. 1992, *ApJ*, **387**, L55.
Solomon, P.M., & Sage, L.J. 1988, *ApJ*, **334**, 613.
Solomon, P.M., Rivolo, A.R., Barrett, J.W., & Yahil, A. (1987), *ApJ*, **319**, 730.
Solomon, P.M., & Wickramasinghe, N.C. 1969 *ApJ*, **158**, 449.
Wilson, R.W., Jefferts, K.B., & Penzias, A. 1970, *ApJ*, **158**, L43.